International Journal of Computer Information Systems and Industrial Management Applications
ISSN 2150-7988 Volume 18(9s) 2026 pp. 610-623
https://doi.org/10.70917/ijcisim-2026-3459
Article

Predictive Bounded-Deferral Checkpoint Scheduling Under Bandwidth Volatility: An LSTM-Guided Latency and Stability Analysis

Suhel Ahmed Khan[1], Harsh Mathur[2], Jagdish Makhijani[3]

[1] Department of Computer Applications, Rustamji Institute of Technology, BSF Academy, Tekanpur, Gwalior, Madhya Pradesh, India.
ORCID: 0009-0009-5385-8709
Email: suhel@rjit.ac.in
[2] Department of Computer Science & Engineering, Rabindranath Tagore University, Raisen, Madhya Pradesh, India.
ORCID: 0000-0002-5726-0861
[3] Department of Computer Science & Engineering, Rustamji Institute of Technology, BSF Academy, Tekanpur, Gwalior, Madhya Pradesh, India.
ORCID: 0000-0002-3601-3319
Corresponding Author:
Suhel Ahmed Khan
Email: suhel@rjit.ac.in

Abstract: Checkpointing remains a central rollback-recovery mechanism for large-scale distributed execution, but the cost of a coordinated checkpoint is strongly coupled to the communication conditions at the instant at which checkpoint traffic is released. Fixed-period policies ignore this coupling, whereas reactive policies may act on a bandwidth observation that is already stale when the next checkpoint cycle begins. This study reformulates checkpoint initiation as a bounded-deferral control problem and proposes Predictive Bounded-Deferral Checkpointing (PBDC), an LSTM-guided scheduler that forecasts one-step-ahead bandwidth and either executes a due checkpoint, postpones it for a short re-evaluation interval, or forces execution when a reliability-preserving deferral budget is exhausted. A risk-sensitive objective combining expected cycle time, cycle-time variance, and deferral cost is developed, together with an analytical condition under which a one-step deferral is latency-beneficial. The approach is related to, but does not replace, classical Young-Daly checkpoint-period selection: the base checkpoint frequency remains reliability-driven, while PBDC shifts checkpoint initiation only within bounded temporal slack. Using the reported 1,000-process MPI simulation summaries of 1,000 cycles per strategy and 2,000,000 timing observations, the forecast-guided policy achieves a mean cycle time of 2.45 on the simulator timing scale, compared with 2.96 for reactive adaptation and 2.81 for static scheduling. Relative to the reactive baseline, mean cycle time decreases by 17.2%, standard deviation by 41.9%, variance by 66.3%, and maximum observed cycle time by 24.8%. Under an independent-cycle approximation, summary-statistics analysis gives Welch $t \approx 44.99$ and Cohen's $d \approx 2.01$ for PBDC versus the reactive baseline. The results support forecast-guided checkpoint timing as a practical mechanism for reducing both latency and instability; they also identify prediction calibration, wall-clock validation, and multi-feature network sensing as necessary next steps for production deployment..

Keywords: distributed systems; checkpointing; rollback recovery; LSTM; bandwidth forecasting; bounded deferral; latency stability; MPI..

1. INTRODUCTION

Distributed platforms increasingly execute scientific simulations, cloud services, data analytics, stream-processing pipelines, and large artificial-intelligence workloads across hundreds or thousands of processes. At these

scales, failure handling is not an auxiliary implementation detail. A process, node, network path, or storage component may fail during a long-running job, and the system must preserve useful work without forcing complete re-execution. Checkpoint/restart therefore continues to be one of the most widely used recovery mechanisms in message-passing and high-performance computing environments [1]–[3].

The classical checkpointing literature primarily asks two questions: how to construct a consistent recoverable state and how often that state should be stored. Coordinated checkpointing prevents the domino effect by ensuring that participating processes form a consistent global checkpoint [2], [3]. Period-selection models, including the Young and Daly formulations, balance checkpoint overhead against expected recomputation after failures [4], [7], [8]. These foundations remain important, but contemporary distributed systems expose another source of variability: the cost of creating the checkpoint can change substantially from one checkpoint opportunity to the next because network and I/O conditions are time varying.

Network volatility is especially relevant when a coordinated checkpoint causes simultaneous state movement from many workers. Congestion, co-located traffic, virtualized network interference, routing variation, bursty application communication, and storage back-pressure can reduce effective transfer throughput. A checkpoint initiated during a temporary bandwidth trough can take longer than an otherwise identical checkpoint initiated shortly afterward. Modern checkpointing systems have therefore explored multi-level storage, memory-resident checkpoints, asynchronous persistence, write-path optimization, and runtime tuning [10]–[18]. These systems confirm that checkpoint performance is tightly coupled to the communication and storage path.

Existing adaptive schemes improve over fixed behavior by observing the current system state. However, current-state adaptation is still reactive. Let a bandwidth sample be collected at time t and let a checkpoint decision take effect at $t+\delta$. When bandwidth varies on a comparable time scale, $B(t)$ may be a poor surrogate for $B(t+\delta)$. The decision then suffers from reaction lag: the system responds correctly to an observation that no longer describes the execution interval. The earlier smart-interval checkpointing work of Makhijani et al. [5] showed the value of restricting checkpoint actions to favorable logical intervals, while the bandwidth-focused study of Khan et al. [6] directly motivated the distinction between static and dynamic network conditions. The present work develops this line of reasoning by replacing current-state timing with forecast-guided bounded deferral.

We propose Predictive Bounded-Deferral Checkpointing (PBDC). A checkpoint remains due according to a base reliability policy; PBDC does not indefinitely postpone recovery protection. Instead, the coordinator uses a short-horizon LSTM forecast to estimate the bandwidth available for the imminent checkpoint cycle. If the forecast indicates an acceptable transmission window, the checkpoint is executed. Otherwise, the scheduler waits for a short re-evaluation interval and repeats inference until either a favorable forecast appears or a maximum deferral budget is reached. The bounded budget is the key reliability safeguard: prediction can optimize timing, but it cannot disable checkpointing.

The paper also addresses a methodological weakness that often appears in adaptive-scheduling studies: reporting only a mean latency improvement. In distributed systems, variance and tail behavior are operationally important because a small number of slow checkpoint cycles can create synchronization stalls or timeout cascades. We therefore model a risk-sensitive objective that jointly considers expected cycle cost, variance, and deferral. The available cycle summaries are re-analyzed with confidence intervals, coefficient of variation, effect size, and an explicit correction of the earlier terminology: a reduction from 0.31 to 0.18 is a 41.9% reduction in standard deviation but a 66.3% reduction in variance.

The principal contributions are fourfold. First, checkpoint start-time selection is formulated as a bounded-deferral control problem that is complementary to classical checkpoint-period selection. Second, an LSTM-guided execute/defer policy is defined with an explicit reliability deadline and a latency-benefit condition for one-step deferral. Third, the study introduces a risk-sensitive evaluation that separates mean reduction, standard-deviation reduction, variance reduction, and maximum-cycle reduction. Fourth, the existing 1,000-process simulation summaries are subjected to a transparent statistical re-analysis, and the limitations of simulator-scale timing and missing forecast-calibration statistics are stated explicitly rather than hidden.

2. BACKGROUND AND RELATED WORK

2.1 Coordinated checkpointing and checkpoint-period selection

Rollback-recovery protocols have been systematically classified into checkpoint-based and log-based families [1]. Distributed snapshots provide a formal mechanism for reasoning about consistent global state [2], and coordinated

checkpointing protocols subsequently reduced unnecessary checkpoint participation while preserving consistency [3]. Early recovery work also examined optimistic message logging, checkpointing in mobile systems, and adaptive fault-tolerant execution [35]–[37].

Checkpoint frequency has a direct performance-reliability trade-off. Young derived a first-order approximation to the checkpoint interval [4], and Daly developed a higher-order estimate that better models restart behavior [7]. Later work clarified the assumptions behind Young-Daly checkpointing and showed that a single formula is not universally optimal across workflows, shared platforms, multilevel checkpointing, and prediction-aware systems [8], [38]. PBDC is not presented as a replacement for these period-selection models. It operates at a different layer: once a checkpoint is due, PBDC selects a nearby execution opportunity within a bounded slack window.

2.2 Adaptive, multilevel, and modern checkpoint systems

The smart-interval protocol of Makhijani et al. [5] reduces checkpoint and message-logging overhead by constraining checkpoint formation to a suitable interval. More recent mathematical and systems work has optimized multilevel checkpoint selection, incorporated failure prediction, and dynamically tuned fault-tolerance configurations [11]–[13]. These studies demonstrate that the best checkpoint behavior depends on observed platform characteristics rather than a single static configuration.

At the systems level, Open MPI checkpoint/restart integrated recovery with the runtime [9], while scalable multilevel designs such as SCR reduced pressure on global storage [10]. Storage and write-path optimization remain active topics: LSM-tree-based checkpoint writes improve sequential access characteristics [18], and memory-centric or asynchronous checkpoint designs reduce the recovery or persistence bottleneck. In large-model training, Gemini uses in-memory checkpoints and communication scheduling [14]; just-in-time checkpointing minimizes lost work after training failures [15]; FlowCheck decouples checkpointing from model training [16]; and LowDiff uses low-cost differential checkpoints for frequent protection [17]. These systems are workload-specific in several respects, but they reinforce a common observation: where and when checkpoint traffic is injected matters.

2.3 Forecasting network and cloud time series

LSTM networks were introduced to address vanishing-gradient limitations in recurrent sequence learning and remain widely used for temporally dependent data [19]. Network-traffic prediction studies have applied recurrent models to communication traces [20], while cloud-workload forecasting has used deep learning to identify turning points and nonlinear temporal patterns [21]–[24]. Recent evaluations also caution that model complexity alone does not guarantee better multi-step forecasting; performance depends on horizon, domain, data quantity, and volatility [25], [26].

A second issue is uncertainty. A point forecast can be accurate on average yet unreliable at precisely the high-volatility moments that drive a control decision. Quantile and uncertainty-aware forecasting frameworks therefore estimate prediction intervals rather than only means [27], [28]. Conformalized quantile regression offers finite-sample coverage under exchangeability assumptions [29], while Monte Carlo dropout and deep ensembles provide alternative uncertainty estimates [30], [31]. The present experiment uses a point LSTM forecast because that is what the available simulation implementation reports; uncertainty-aware execution is discussed as a direct extension rather than claimed as an evaluated component.

2.4 Research gap and positioning

The literature has strong foundations in checkpoint consistency, checkpoint-period optimization, storage-path acceleration, and time-series forecasting. What remains less directly characterized is the use of a short-horizon bandwidth forecast as an input to the start-time decision of a due coordinated checkpoint, subject to an explicit maximum deferral. PBDC focuses on this narrow control point. Table 1 positions the proposed approach against representative strategies.

Table 1. Positioning of PBDC relative to representative checkpointing strategies

Strategy	Decision basis	Bandwidth volatility	Reliability guard	Primary limitation / distinction

Fixed coordinated	Predefined checkpoint period	Not directly modeled	Base period / protocol consistency	Cannot exploit short favorable windows
Reactive adaptive	Current B(t) or observed delay	Partially	Policy dependent	Decision may suffer reaction lag
Smart interval [5]	Logical checkpoint interval	Indirect	Consistent checkpoint interval	No learned short-horizon network forecast
Young-Daly family [4], [7], [8]	Failure rate and checkpoint cost	Usually aggregate cost	Optimal/near-optimal period assumptions	Selects frequency, not imminent start opportunity
Modern storage/training systems [14]–[18]	Storage hierarchy, overlap, write path	Often workload-specific	System-specific recovery design	Primarily optimizes placement/persistence path
PBDC (this study)	Forecast $\hat{B}(t+1)$ + threshold + Dmax	Direct short-horizon treatment	Forced execution at Dmax	Point forecast; calibration not yet evaluated

3. SYSTEM MODEL AND PROBLEM FORMULATION

3.1 Distributed execution model

Let P = {P1, P2, …, Pn} be a set of n communicating processes. One process acts as checkpoint coordinator Pc, although the control logic can be replicated in a production implementation. A checkpoint due time tk is generated by the base checkpoint-period policy. Cohorts create local state, the coordinator collects acknowledgements, and a global checkpoint is committed only after the consistency protocol succeeds. The forecast scheduler is therefore an initiation controller; it does not change the consistency semantics of the coordinated checkpoint.

Let $B_t > 0$ denote the effective bandwidth available to checkpoint traffic at time t, S the aggregate transferable checkpoint state on the modeled path, $\rho_t \in (0,1]$ a protocol-efficiency factor, Tcoord the coordination cost, Tio the storage-side cost, and Tinf the forecast-inference cost. For a checkpoint executed at time t, a simplified cycle-time model is

$$C(t) = T_{coord} + S / (\rho_t B_t) + T_{io} + T_{inf}. \quad (1)$$

Equation (1) intentionally isolates the bandwidth-sensitive term. Real platforms may also include compression, serialization, overlap, burst-buffer staging, retransmission, and topology effects. These can be absorbed into S, ρ_t, or additional cost terms without changing the scheduling argument.

3.2 Reaction lag

A reactive controller samples bandwidth at time t but may initiate the checkpoint at $t+\delta$ because measurement, coordination, or application progress consumes time. We define normalized reaction-lag mismatch as

$$R_{lag}(t, \delta) = |B(t+\delta) - B(t)| / (B(t+\delta) + \varepsilon), \quad \varepsilon > 0. \quad (2)$$

A large Rlag means that the current measurement is a poor proxy for the bandwidth that actually governs checkpoint transfer. The forecast-guided alternative estimates $B(t+\delta)$ from the recent history H_t rather than assuming persistence of B(t).

3.3 Bounded-deferral decision variable

Let $a_t \in \{0,1\}$ be the checkpoint-start action: $a_t = 1$ executes the due checkpoint and $a_t = 0$ defers it by a re-evaluation interval δ. Let D_t be the accumulated deferral since the base due time t_k. The reliability constraint is

$$0 \le D_t \le D_{max}, \quad \text{and} \quad a_t = 1 \text{ whenever } D_t = D_{max}. \quad (3)$$

This constraint separates PBDC from unconstrained opportunistic checkpointing. The method may choose a better communication window, but the added recovery exposure is deterministically bounded by D_{max}.

3.4 Risk-sensitive scheduling objective

Mean checkpoint latency alone is an incomplete objective because high variability can be harmful to synchronized distributed execution. For a policy π, we therefore define

$$J(\pi) = E[C_\pi] + \lambda \, Var(C_\pi) + \gamma \, E[D_\pi], \quad \lambda \ge 0, \gamma \ge 0. \quad (4)$$

The first term rewards low average cycle cost, the second penalizes instability, and the third prevents the scheduler from obtaining low transfer times simply by deferring every difficult cycle. The hard constraint in (3) remains active even when γ is small.

3.5 Forecast model

The coordinator maintains a sliding history window of k bandwidth observations, $H_t = [B(t-k+1), \ldots, B(t)]$. After normalization, an LSTM maps this sequence to a one-step-ahead point forecast

$$\hat{B}(t+1) = f_{LSTM}(H_t; W), \quad (5)$$

where W denotes learned parameters. Training minimizes mean squared forecast error on the training sequence:

$$L_{MSE}(W) = (1/N) \sum_{i=1..N} [B(i+1) - \hat{B}(i+1)]^2. \quad (6)$$

The original simulation configuration uses one recurrent layer with 50 hidden units, a 50-sample input window, a dense scalar output, Adam optimization with learning rate 0.001, 100 epochs, and batch size 32. The forecast is computed only at the coordinator.

Table 2. Principal notation

Symbol	Meaning
n	Number of distributed processes
B_t	Effective bandwidth available to checkpoint traffic at time t
S	Aggregate checkpoint state transferred on the modeled path
ρ_t	Protocol/transfer efficiency factor
t_k	Base checkpoint due time
δ	Re-evaluation interval after one deferral
D_t	Accumulated deferral for the current due checkpoint
D_{max}	Maximum permitted deferral
θ	Safe-transmission bandwidth threshold
$\hat{B}(t+1)$	One-step-ahead LSTM bandwidth forecast
$C(t)$	Checkpoint cycle-time cost
λ, γ	Variance and deferral penalty weights

4. PREDICTIVE BOUNDED-DEFERRAL CHECKPOINTING

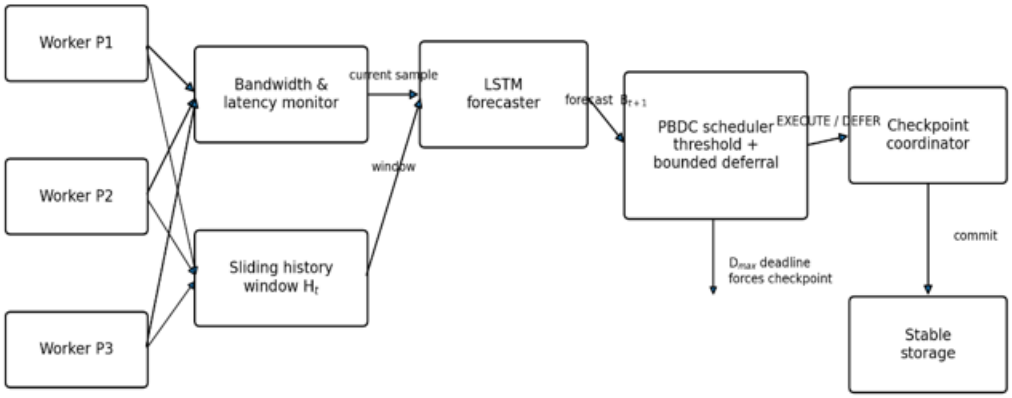

Fig. 1. PBDC architecture: monitoring and history feed a one-step LSTM forecast, which is converted into an execute/defer action subject to a maximum deferral deadline.

4.1 Offline training and online control

PBDC has an offline forecasting phase and an online scheduling phase. During offline preparation, historical bandwidth samples are ordered chronologically, normalized using parameters estimated only from the training portion, and transformed into sliding windows of length k. The LSTM is trained to predict the next sample. Chronological splitting is preferable to random shuffling for time-series evaluation because it avoids leaking future patterns into the training sequence.

During online execution, the coordinator appends the latest bandwidth sample to Ht and performs a single forward pass. A due checkpoint is executed when the forecast satisfies $\hat{B}(t+1) \geq \theta$. Otherwise, the checkpoint is deferred by δ and re-evaluated. When accumulated deferral reaches Dmax, the coordinator executes regardless of the forecast. The result is a three-state interpretation: execute under predicted safe bandwidth, defer under predicted congestion, and force execution at the reliability deadline.

4.2 Decision rule

$a_t = 1$, if $\hat{B}(t+1) \geq \theta$ or $D_t \geq D_{max}$; $a_t = 0$, otherwise. (7)

A fixed θ is used in the reported implementation. In a production deployment, θ should be selected on validation data or derived from a service-level constraint. Importantly, θ is a scheduling threshold, not a claim that all bandwidth above θ is congestion-free.

4.3 Algorithm

Algorithm 1. Predictive Bounded-Deferral Checkpointing (PBDC)

Input: due checkpoint at t_k, history Ht, trained LSTM fLSTM, threshold θ, re-evaluation interval δ, maximum deferral Dmax.

1. Set $D \leftarrow 0$.

2. Measure the latest bandwidth sample and append it to Ht.

3. Compute $\hat{B}(t+1) \leftarrow$ fLSTM(Ht).

4. If $\hat{B}(t+1) \geq \theta$ or $D \geq D_{max}$, broadcast PREPARE and initiate the coordinated checkpoint.

5. Otherwise, wait δ, set $D \leftarrow D + \delta$, and return to Step 2.

6. Collect cohort acknowledgements, commit the global checkpoint, and record cycle cost and forecast residual.

7. Continue with the base checkpoint-period policy for the next due checkpoint.

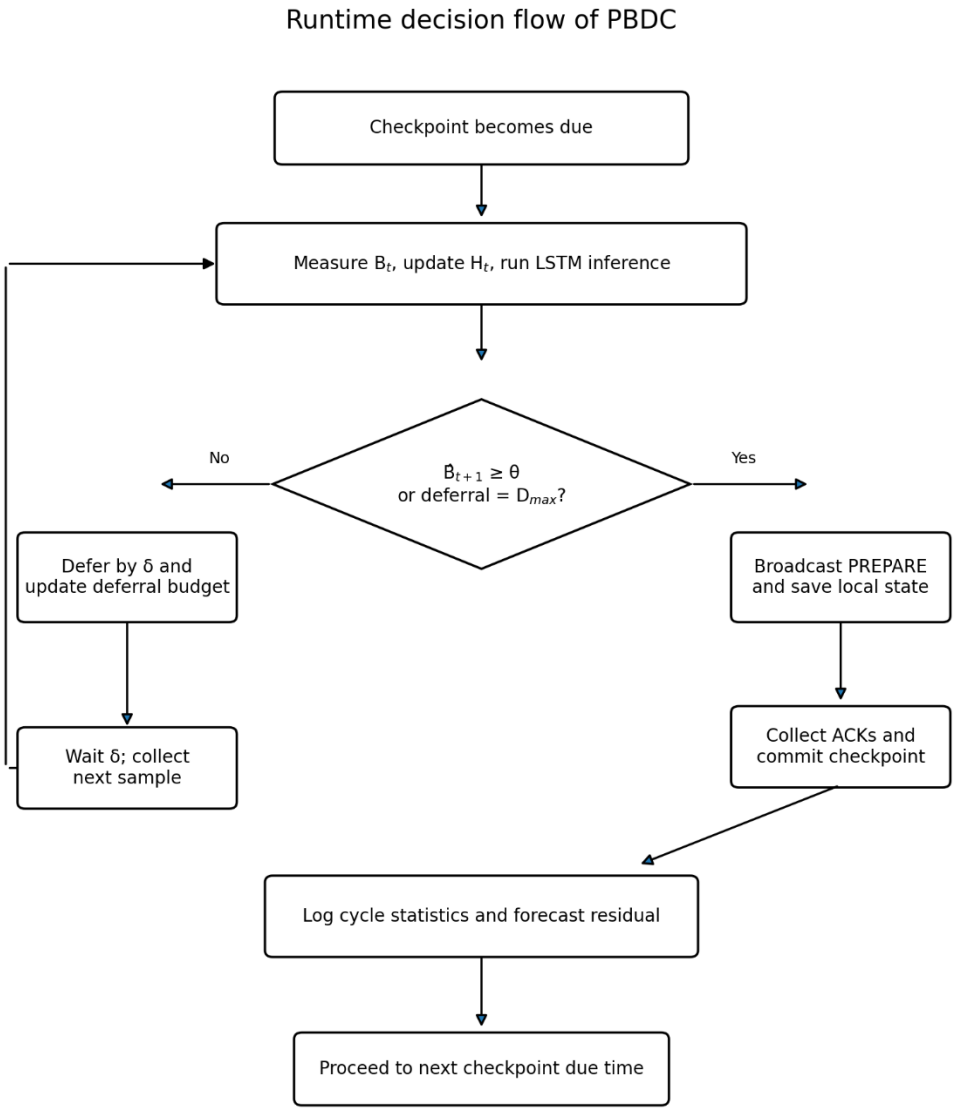

Fig. 2. Runtime decision flow of the proposed PBDC scheduler.

5. ANALYTICAL PROPERTIES

5.1 One-step latency-benefit condition

Consider a due checkpoint for which the coordinator can either execute now or defer by one interval δ. Ignoring terms common to both choices and using forecasted effective bandwidths $\hat{B}t$ and $\hat{B}t+1$, immediate execution has approximate cost $S/(\rho\hat{B}t)$, while one-step deferral has cost $\delta + Tinf + S/(\rho\hat{B}t+1)$. Deferral is latency-beneficial when

$$\delta + Tinf < (S/\rho)\,[1/\hat{B}t - 1/\hat{B}(t+1)]. \quad (8)$$

Equation (8) gives a direct economic interpretation of forecast-guided scheduling. A higher future bandwidth is not sufficient by itself; the predicted transfer-time saving must exceed the waiting and inference cost. The threshold rule in (7) is a lightweight implementation of this broader cost comparison.

5.2 Bounded recovery exposure

Let the base checkpoint policy schedule a checkpoint at tk. From (3), PBDC executes no later than tk + Dmax. Therefore, relative to the base policy, the additional interval of potentially lost computation caused by checkpoint timing is upper bounded by Dmax. This simple bound is important because a predictor can be inaccurate or encounter a distribution shift; the checkpoint deadline remains independent of forecast quality.

5.3 Transfer-time upper bound for non-forced cycles

For a non-forced cycle executed only when the realized bandwidth satisfies $B(t) \geq \theta$, the bandwidth-sensitive transfer term in (1) obeys

$$T_{transfer}(t) = S/(\rho_t B(t)) \leq S/(\rho_{min} \theta), \quad (9)$$

provided $\rho_t \geq \rho_{min} > 0$. Equation (9) explains why avoiding the lower bandwidth tail can reduce the maximum and dispersion of checkpoint cycle time. The bound does not hold for a forced cycle at Dmax, which is deliberately retained to preserve recovery protection.

5.4 Expected deferral under a simplified opportunity model

For intuition, suppose each re-evaluation independently produces a favorable forecast with probability p, and at most $m = D_{max}/\delta$ deferrals are allowed. Let N be the number of deferrals. With $q = 1 - p$,

$$E[N] = \Sigma_{j=1..m} P(N \geq j) = \Sigma_{j=1..m} q^j = q(1 - q^m)/p. \quad (10)$$

$$E[D] = \delta \cdot q(1 - q^m)/p. \quad (11)$$

This simplified model is not used to generate the reported results; consecutive bandwidth samples are generally correlated. It nevertheless shows the design trade-off: a high threshold can reduce transmission cost but lowers p and increases expected waiting. Threshold selection should therefore be performed jointly with Dmax and δ.

5.5 Relationship to Young-Daly period selection

Under classical assumptions, the Young-Daly family approximates a checkpoint period using failure mean time and checkpoint cost, with the familiar first-order form $W \approx \sqrt{(2\mu C)}$ [4], [7], [8]. PBDC should be placed downstream of such a period selector. The base policy determines when protection is due; PBDC searches only the interval [tk, tk + Dmax] for a better transfer opportunity. A conservative deployment chooses Dmax much smaller than the base checkpoint period W, so short-term network optimization does not dominate the long-term reliability schedule.

6. EXPERIMENTAL METHODOLOGY

6.1 Simulation configuration

The evaluation reuses the controlled MPI-based simulation configuration reported in the source study. The system contains 1,000 concurrent processes. Static coordinated checkpointing, reactive adaptive checkpointing, and the forecast-guided policy are each evaluated over 1,000 checkpoint cycles. The aggregated instrumentation contains 2,000,000 timing observations. The LSTM uses 50 hidden units and a 50-sample input window; optimization uses Adam with learning rate 0.001, mean squared error loss, 100 epochs, and batch size 32.

The available aggregate file reports checkpoint-cycle values on a microsecond-labelled simulator scale. Because the experiment is simulation-based and the provided summary does not include an external wall-clock calibration trace, the analysis below emphasizes relative differences among strategies. This distinction is important: the values should not be interpreted as end-to-end production checkpoint durations for a 1,000-process cluster until the simulator unit and timing instrumentation are independently validated.

Table 3. Experimental and analytical configuration

Parameter	**Value**
Distributed processes	1,000
Checkpoint cycles per strategy	1,000
Aggregate timing observations	2,000,000

Compared strategies	Static; reactive adaptive; PBDC
Forecast model	Single-layer LSTM, 50 hidden units
Input window	50 samples
Optimizer	Adam; learning rate 0.001
Loss	Mean squared error
Training	100 epochs; batch size 32
Primary outcomes	Mean, standard deviation, variance, maximum cycle time
Statistical re-analysis	Approximate 95% CI, Welch t, Cohen's d, coefficient of variation

6.2 Baselines

The static baseline follows a fixed coordinated-checkpoint schedule and does not alter checkpoint timing in response to bandwidth variation. It represents a predictable but network-unaware policy.

The reactive adaptive baseline uses currently observed communication conditions to alter checkpoint behavior. Its purpose is to represent an adaptive method that reacts after a condition has been measured. It is therefore vulnerable to the mismatch in (2) when conditions evolve between measurement and execution.

PBDC uses the same checkpointing semantics but replaces the current-state timing signal with the one-step LSTM forecast and the bounded-deferral rule in (7). No additional worker-side neural model is deployed.

6.3 Metrics and statistical re-analysis

For strategy s with ns checkpoint cycles, let Csi denote cycle time, $\bar{C}s$ the sample mean, and ss the sample standard deviation. We compute coefficient of variation CVs = 100 ss/$\bar{C}s$, approximate standard error SEs = ss/$\sqrt{ns}$, and a normal-approximation 95% confidence interval $\bar{C}s \pm 1.96SEs$. For PBDC and the reactive baseline, Welch's summary-statistics t value is calculated from the reported means, standard deviations, and n = 1,000 cycles per strategy. Cohen's d uses the pooled standard deviation. These inferential calculations assume approximately independent cycle-level observations; because raw logs are not available in the manuscript package, the results are reported as a summary-statistics re-analysis rather than a substitute for a blocked bootstrap or autocorrelation-aware test on the original trace.

7. RESULTS AND STATISTICAL ANALYSIS

7.1 Comparative checkpoint performance

Table 4 summarizes the reported cycle statistics. PBDC has the lowest mean, standard deviation, and maximum cycle time. The reactive baseline is slower and more variable than the static baseline in this simulation, which is consistent with the reaction-lag hypothesis: adaptation based on a stale observation can be worse than a stable fixed decision.

Table 4. Comparative latency and stability statistics on the reported simulator timing scale

Model	**Mean cycle time**	**Std. deviation**	**Variance**	**Maximum cycle time**	**CV (%)**
Static	2.81	0.23	0.0529	3.20	8.19
Reactive adaptive	2.96	0.31	0.0961	3.43	10.47
PBDC	2.45	0.18	0.0324	2.58	7.35

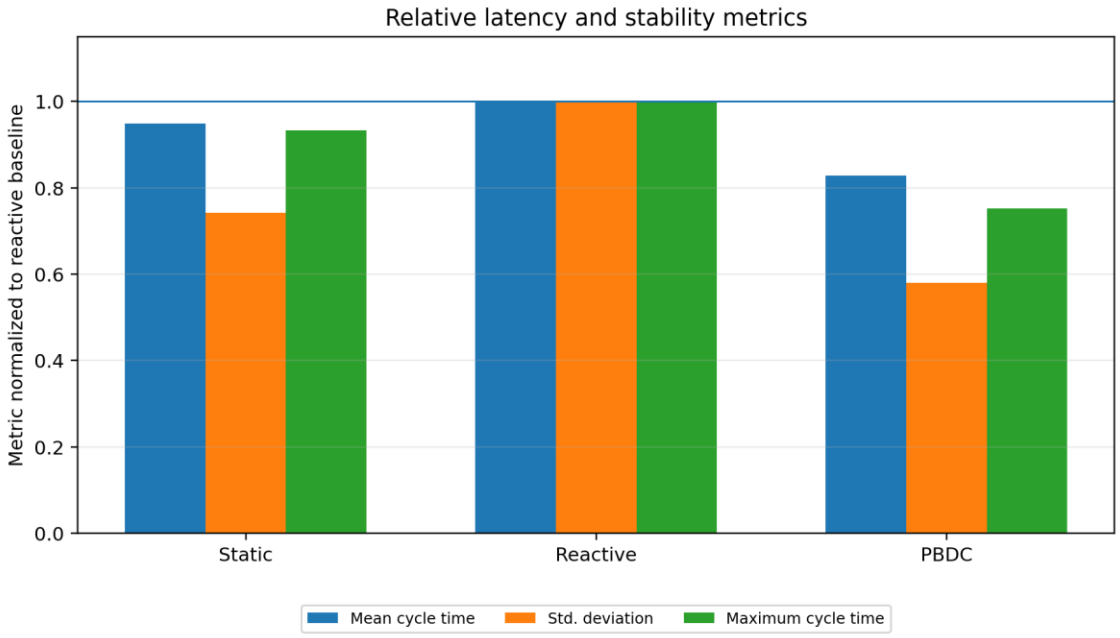

Fig. 3. Mean, standard deviation, and maximum cycle time normalized to the reactive baseline (reactive = 1.0).

7.2 Corrected interpretation of dispersion reduction

Relative to the reactive baseline, mean cycle time falls from 2.96 to 2.45, giving a reduction of 17.23%. The standard deviation falls from 0.31 to 0.18, a reduction of 41.94%. The earlier manuscript used the term "variance reduction" for this 41.9% value; mathematically, that terminology is incorrect because variance is the square of the standard deviation. The variance decreases from 0.0961 to 0.0324, corresponding to a 66.29% variance reduction. The maximum observed cycle time decreases from 3.43 to 2.58, or 24.78%.

$$\text{Mean reduction} = 100(1 - 2.45/2.96) = 17.23\%. \quad (12)$$

$$\text{SD reduction} = 100(1 - 0.18/0.31) = 41.94\%. \quad (13)$$

$$\text{Variance reduction} = 100[1 - (0.18^2/0.31^2)] = 66.29\%. \quad (14)$$

$$\text{Maximum-cycle reduction} = 100(1 - 2.58/3.43) = 24.78\%. \quad (15)$$

The coefficient of variation also improves: 10.47% for reactive adaptation, 8.19% for static scheduling, and 7.35% for PBDC. Thus, the forecast-guided policy improves not only absolute cycle time but relative stability.

7.3 Approximate confidence intervals and effect size

Table 5. Summary-statistics confidence intervals and relative dispersion

Strategy	**Mean**	**SE**	**Approx. 95% CI**	**CV (%)**
Static	2.81	0.00727	[2.7957, 2.8243]	8.19
Reactive adaptive	2.96	0.00980	[2.9408, 2.9792]	10.47
PBDC	2.45	0.00569	[2.4388, 2.4612]	7.35

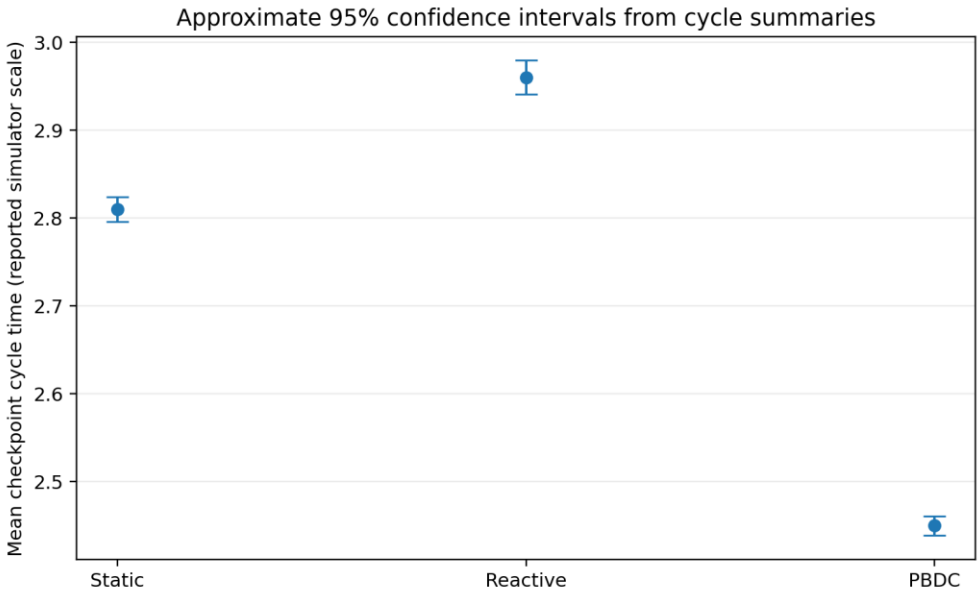

Fig. 4. Approximate 95% confidence intervals derived from the reported cycle summaries and n = 1,000 cycles per strategy.

Using the reported means and standard deviations with n = 1,000 cycles per strategy, the approximate Welch comparison between reactive adaptation and PBDC is $t \approx 44.99$ with approximately 1,604 degrees of freedom. The corresponding pooled-standard-deviation effect size is Cohen's $d \approx 2.01$. Under the independent-cycle approximation, this is a very large standardized separation. Because distributed timing traces can be autocorrelated, the effect size is more informative here than a nominal p-value that would become extremely small at n = 1,000. A final submission should repeat the comparison on the raw logs using a block bootstrap or a time-series-aware resampling procedure.

7.4 Practical meaning of the result

The result supports the central scheduling hypothesis: a checkpoint coordinator can benefit from treating near-future communication capacity as a decision variable. PBDC does not reduce the amount of state that must eventually be checkpointed. Instead, it changes the time at which the transfer is allowed to contend for the network. This distinction explains why the primary benefit appears in both mean and dispersion.

The lower maximum cycle time is particularly relevant to synchronized workloads. A coordinated checkpoint can hold fast processes while slow participants complete their state transfer. Reducing the slowest cycle in the evaluated sample by 24.8% therefore has practical value beyond the average 17.2% reduction, although the simulator does not model every source of real cluster straggling.

The reactive baseline performing worse than the static baseline should not be generalized to all adaptive checkpointing. It shows only that the particular reactive timing mechanism used in the simulation is vulnerable to reaction lag under the generated volatility pattern. More sophisticated reactive policies, control-theoretic approaches, and storage-aware schedulers remain important baselines for future implementation-level evaluation.

8. DISCUSSION

8.1 Why bounded deferral is preferable to unconstrained opportunism

A forecast scheduler that waits indefinitely for ideal bandwidth is not a fault-tolerance mechanism; it trades away recoverability for a low transfer time. PBDC explicitly prevents this failure mode through Dmax. This design also provides a clean fallback when the LSTM encounters concept drift, a sudden traffic regime change, or an adversarially poor sequence: once the deferral budget is consumed, the checkpoint proceeds.

8.2 Forecast accuracy versus decision quality

A low MSE does not automatically imply a good checkpoint decision. The scheduler ultimately cares whether the forecast places the next interval on the correct side of θ and whether the predicted transfer saving exceeds the deferral cost in (8). Therefore, future experiments should report both forecasting metrics (MAE, RMSE, MAPE where meaningful) and control metrics (wrong-deferral rate, missed-opportunity rate, forced-checkpoint ratio, accumulated deferral, and end-to-end job completion time). This distinction is consistent with the broader forecasting literature, which warns that point-error metrics alone can be insufficient for operational decisions [25]–[29].

8.3 Uncertainty-aware extension

The present PBDC implementation uses $\hat{B}(t+1)$ as a point estimate. A risk-averse extension can replace the decision in (7) with a calibrated lower prediction bound $L\alpha(t+1)$. The checkpoint executes only if $L\alpha(t+1) \geq \theta$ or the deadline is reached. Quantile or conformal methods can construct such bounds [27]–[29], while epistemic uncertainty can be estimated using Monte Carlo dropout or ensembles [30], [31]. This extension would make the decision conservative precisely when the predictor is uncertain, but it requires separate calibration experiments and is not included in the reported performance numbers.

$$a_t = 1 \text{ if } L\alpha(t+1) \geq \theta \text{ or } D_t \geq D_{max}; \text{ otherwise } a_t = 0. \quad (16)$$

8.4 Deployment considerations

First, the monitor must measure the bandwidth actually relevant to checkpoint traffic rather than aggregate link capacity. Effective throughput may differ because of protocol overhead, topology, or storage back-pressure. Second, the forecast model should be retrained or adapted when residual drift persists. Third, inference should remain coordinator-local or otherwise amortized; model execution on every worker would add unnecessary synchronization. Fourth, checkpoint size S should be included as an input when checkpoint state varies strongly across cycles. Finally, the base checkpoint period and Dmax should be co-configured so that network optimization cannot materially degrade the recovery point objective.

For heterogeneous systems, a multivariate history H_t could include bandwidth, RTT, retransmission rate, queue depth, storage write throughput, number of active flows, and checkpoint size. Such features would shift the model from bandwidth prediction to direct cycle-cost prediction. The decision condition in (8) remains applicable if $\hat{B}$ is replaced by a predicted checkpoint cost $\hat{C}$.

9. THREATS TO VALIDITY AND REPRODUCIBILITY REQUIREMENTS

9.1 Internal validity

The reported evaluation is simulation-based. The smooth relationship between network condition and cycle cost may be stronger than in a production system with storage contention, CPU scheduling noise, retransmissions, and topology effects. The analysis also relies on aggregate summaries rather than the raw cycle trace. Consequently, the Welch comparison assumes independent cycle-level observations and cannot test autocorrelation. A block bootstrap on raw cycles is required for stronger inference.

9.2 Construct validity

The primary outcome is checkpoint cycle time. This is relevant but incomplete. A complete fault-tolerance evaluation should also report application makespan, rollback work after injected failures, recovery time, checkpoint success rate, deferral ratio, forced-checkpoint ratio, and prediction error. The current dataset does not expose all of these outcomes.

9.3 External validity

The system contains 1,000 simulated MPI processes, which is useful for observing coordination effects but does not represent all production environments. Cloud overlays, Kubernetes networking, heterogeneous NICs, RDMA, burst buffers, object stores, and distributed-training frameworks can exhibit different bottlenecks. The absolute simulator timing scale must therefore be validated against wall-clock measurements before the values are interpreted as production checkpoint duration.

9.4 Reproducibility checklist for the next experimental release

A journal-grade replication package should include: (i) simulator source and commit identifier; (ii) trace-generation equations and random seeds; (iii) exact definition and unit of every timing field; (iv) chronological

train/validation/test split; (v) scaler parameters fitted only on the training set; (vi) LSTM framework and library versions; (vii) per-cycle predictions, forecast residuals, actions, deferral durations, and checkpoint costs; and (viii) scripts that regenerate all tables and figures. The current manuscript deliberately avoids claiming forecast RMSE, inference overhead, or ablation results because those values are not present in the available aggregate source.

10. CONCLUSION

This paper presented Predictive Bounded-Deferral Checkpointing, a forecast-guided start-time controller for coordinated checkpointing under bandwidth volatility. The approach preserves the base checkpoint frequency but allows a due checkpoint to move within a bounded temporal slack window. An LSTM provides a one-step-ahead bandwidth forecast; a threshold rule determines whether to execute or defer; and a hard maximum deferral prevents prediction from undermining recovery protection. The formulation connects checkpoint timing with a risk-sensitive objective that includes mean cost, variance, and waiting penalty, and it yields a simple condition for when one-step deferral is economically justified.

On the reported 1,000-process simulation summaries, the forecast-guided policy reduces mean cycle time by 17.2% relative to reactive adaptation. More importantly, the corrected dispersion analysis shows a 41.9% reduction in standard deviation and a 66.3% reduction in variance, while the maximum observed cycle time decreases by 24.8%. Approximate summary-statistics analysis produces a large standardized effect (Cohen's $d \approx 2.01$). These results support the use of short-horizon communication forecasts in checkpoint-start decisions, while the limitations of simulator-scale timing, aggregate-only statistics, and missing forecast calibration prevent overgeneralization.

Future work should validate PBDC on an instrumented MPI or container cluster, publish raw cycle traces, compare LSTM against GRU, temporal convolution, and Transformer forecasters, and evaluate uncertainty-aware lower-bound decisions. A multivariate cost predictor using RTT, packet loss, queue occupancy, storage throughput, and checkpoint size is a particularly promising extension. The central design principle remains simple: checkpoint frequency should protect reliability, while bounded predictive timing can reduce the cost of executing the checkpoints that reliability requires.

Declarations

Funding: No external funding is declared for this study.

Conflict of interest: The authors declare no conflict of interest.

Author contributions: S.A.K. contributed to conceptualization, simulation framing, and manuscript preparation; Harsh and J.M. contributed to supervision, checkpointing methodology, and technical review.

References:

1. E. N. Elnozahy, L. Alvisi, Y.-M. Wang, and D. B. Johnson, “A survey of rollback-recovery protocols in message-passing systems,” ACM Computing Surveys, vol. 34, no. 3, pp. 375–408, 2002. doi: 10.1145/568522.568525.
2. K. M. Chandy and L. Lamport, “Distributed snapshots: Determining global states of distributed systems,” ACM Transactions on Computer Systems, vol. 3, no. 1, pp. 63–75, 1985. doi: 10.1145/214451.214456.
3. G. Cao and M. Singhal, “On coordinated checkpointing in distributed systems,” IEEE Transactions on Parallel and Distributed Systems, vol. 9, no. 12, pp. 1213–1225, 1998. doi: 10.1109/71.737697.
4. J. W. Young, “A first order approximation to the optimum checkpoint interval,” Communications of the ACM, vol. 17, no. 9, pp. 530–531, 1974. doi: 10.1145/361147.361115.
5. J. Makhijani, M. K. Niranjan, M. Motwani, A. K. Sachan, and A. Rajput, “An efficient protocol using smart interval for coordinated checkpointing,” in Information Technology and Mobile Communication, CCIS, vol. 147, pp. 6–12, Springer, 2011. doi: 10.1007/978-3-642-20573-6_2.
6. S. A. Khan, H. Mathur, and J. Makhijani, “Evaluating the impact of static and dynamic network bandwidth on checkpointing-based fault tolerance in distributed systems,” Taylor & Francis conference proceedings, 2026. [Publication metadata/DOI to be verified before submission.]
7. J. T. Daly, “A higher order estimate of the optimum checkpoint interval for restart dumps,” Future Generation Computer Systems, vol. 22, no. 3, pp. 303–312, 2006. doi: 10.1016/j.future.2004.11.016.
8. A. Benoit, Y. Du, T. Hérault, L. Marchal, G. Pallez, L. Perotin, Y. Robert, H. Sun, and F. Vivien, “Checkpointing à la Young/Daly: An overview,” in Proc. 14th Int. Conf. Contemporary Computing (IC3), 2022, pp. 701–710. doi: 10.1145/3549206.3549328.
9. J. Hursey, J. M. Squyres, T. I. Mattox, and A. Lumsdaine, “The design and implementation of checkpoint/restart process fault tolerance for Open MPI,” in Proc. IEEE IPDPS, 2007, pp. 1–8. doi: 10.1109/IPDPS.2007.370605.
10. A. Moody, G. Bronevetsky, K. Mohror, and B. R. de Supinski, “Design, modeling, and evaluation of a scalable multi-level checkpointing system,” in Proc. ACM/IEEE SC, 2010. doi: 10.1109/SC.2010.18.

11. S. Di, M. S. Bouguerra, L. Bautista-Gomez, and F. Cappello, “Optimization of multi-level checkpoint model for large scale HPC applications,” in Proc. IEEE IPDPS, 2014, pp. 1181–1190. doi: 10.1109/IPDPS.2014.122.
12. G. Aupy, Y. Robert, F. Vivien, and D. Zaidouni, “Checkpointing algorithms and fault prediction,” Journal of Parallel and Distributed Computing, vol. 74, no. 2, pp. 2048–2064, 2014. doi: 10.1016/j.jpdc.2013.10.010.
13. M. K. Geldenhuys, B. J. J. Pfister, D. Scheinert, L. Thamsen, and O. Kao, “Khaos: Dynamically optimizing checkpointing for dependable distributed stream processing,” in Proc. FedCSIS, 2022, pp. 553–561. doi: 10.15439/2022F225.
14. Z. Wang, Z. Jia, S. Zheng, Z. Zhang, X. Fu, T. S. E. Ng, and Y. Wang, “GEMINI: Fast failure recovery in distributed training with in-memory checkpoints,” in Proc. 29th ACM Symposium on Operating Systems Principles (SOSP), 2023, pp. 364–381. doi: 10.1145/3600006.3613145.
15. T. Gupta, S. Krishnan, R. Kumar, A. Vijeev, B. S. Gulavani, N. Kwatra, R. Ramjee, and M. Sivathanu, “Just-In-Time Checkpointing: Low cost error recovery from deep learning training failures,” in Proc. EuroSys, 2024, pp. 1110–1125. doi: 10.1145/3627703.3650085.
16. Z. Huang, H. Nie, H. Jia, B. Jiang, J. Guo, J. Lu, R. Wen, B. Lyu, S. Zhu, and X. Wang, “FlowCheck: Decoupling checkpointing and training of large-scale models,” in Proc. EuroSys, 2025, pp. 1334–1349. doi: 10.1145/3689031.3696088.
17. C. Yao, Y. Hu, F. Liu, Z. Liu, and D. Feng, “LowDiff: Efficient frequent checkpointing via low-cost differential for high-performance distributed training systems,” in Proc. SC, 2025, pp. 1113–1126. doi: 10.1145/3712285.3759891.
18. S. Bulut and S. A. Wright, “Optimizing write performance for checkpointing to parallel file systems using LSM-trees,” in Proc. SC-W, 2023, pp. 492–501. doi: 10.1145/3624062.3624118.
19. S. Hochreiter and J. Schmidhuber, “Long short-term memory,” Neural Computation, vol. 9, no. 8, pp. 1735–1780, 1997. doi: 10.1162/neco.1997.9.8.1735.
20. R. Vinayakumar, K. P. Soman, and P. Poornachandran, “Applying deep learning approaches for network traffic prediction,” in Proc. IEEE ICACCI, 2017, pp. 1222–1228. doi: 10.1109/ICACCI.2017.8126078.
21. L. Ruan et al., “Cloud workload turning points prediction via cloud feature-enhanced deep learning,” IEEE Transactions on Cloud Computing, vol. 11, no. 2, pp. 1719–1732, 2023. doi: 10.1109/TCC.2022.3160228.
22. A. Lackinger, A. Morichetta, and S. Dustdar, “Time series predictions for cloud workloads: A comprehensive evaluation,” in Proc. IEEE SOSE, 2024, pp. 36–45. doi: 10.1109/SOSE62363.2024.00011.
23. Z. Ahamed et al., “Technical study of deep learning in cloud computing for workload prediction,” Electronics, vol. 12, no. 3, art. 650, 2023. doi: 10.3390/electronics12030650.
24. K. Valarmathi and K. S. Suresh, “Resource utilization prediction technique in cloud using deep learning models,” Simulation, vol. 98, no. 5, pp. 379–395, 2022. doi: 10.1177/1063293X211032622.
25. S. Saha, A. Haque, and G. Sidebottom, “Overcoming data limitations in internet traffic forecasting: LSTM models with transfer learning and wavelet augmentation,” arXiv:2409.13181, 2024. doi: 10.48550/arXiv.2409.13181.
26. K. Yalda, D. J. Hamad, N. Tapus, and I. Okumus, “Network traffic prediction performance using LSTM,” Romanian Journal of Information Science and Technology, vol. 27, no. 3–4, pp. 336–347, 2024. doi: 10.59277/ROMJIST.2024.3-4.07.
27. Y. Wu, Y. Ye, A. Zeb, J. J. Q. Yu, and Z. Wang, “Adaptive modeling of uncertainties for traffic forecasting,” IEEE Transactions on Intelligent Transportation Systems, vol. 25, no. 5, pp. 4427–4442, 2024. doi: 10.1109/TITS.2023.3327100.
28. W. Qian, D. Zhang, Y. Zhao, K. Zheng, and J. J. Q. Yu, “Uncertainty quantification for traffic forecasting: A unified approach,” in Proc. IEEE ICDE, 2023, pp. 992–1004. doi: 10.1109/ICDE55515.2023.00081.
29. Y. Romano, E. Patterson, and E. J. Candès, “Conformalized quantile regression,” in Advances in Neural Information Processing Systems, vol. 32, 2019, pp. 3538–3548.
30. Y. Gal and Z. Ghahramani, “Dropout as a Bayesian approximation: Representing model uncertainty in deep learning,” in Proc. ICML, 2016, pp. 1050–1059.
31. B. Lakshminarayanan, A. Pritzel, and C. Blundell, “Simple and scalable predictive uncertainty estimation using deep ensembles,” in Advances in Neural Information Processing Systems, vol. 30, 2017.
32. R. J. Hyndman and G. Athanasopoulos, Forecasting: Principles and Practice, 3rd ed. Melbourne, Australia: OTexts, 2021.
33. I. Goodfellow, Y. Bengio, and A. Courville, Deep Learning. Cambridge, MA, USA: MIT Press, 2016.
34. T. G. Dietterich, “Approximate statistical tests for comparing supervised classification learning algorithms,” Neural Computation, vol. 10, no. 7, pp. 1895–1923, 1998. doi: 10.1162/089976698300017197.
35. D. B. Johnson and W. Zwaenepoel, “Recovery in distributed systems using optimistic message logging and checkpointing,” Journal of Algorithms, vol. 11, no. 3, pp. 462–491, 1990. doi: 10.1016/0196-6774(90)90035-F.
36. R. Prakash and M. Singhal, “Low-cost checkpointing and failure recovery in mobile computing systems,” IEEE Transactions on Parallel and Distributed Systems, vol. 7, no. 10, pp. 1035–1048, 1996. doi: 10.1109/71.539738.
37. S. Gorender, R. J. A. Macedo, and M. Raynal, “An adaptive programming model for fault-tolerant distributed computing,” IEEE Transactions on Dependable and Secure Computing, vol. 4, no. 1, pp. 18–31, 2007. doi: 10.1109/TDSC.2007.1003.
38. L. Bautista-Gomez, A. Benoit, S. Di, T. Hérault, Y. Robert, and H. Sun, “A survey on checkpointing strategies: Should we always checkpoint à la Young/Daly?,” Future Generation Computer Systems, vol. 161, pp. 315–328, 2024. doi: 10.1016/j.future.2024.07.022.

.